Research Results

Tri Band Low Profile Closed Loop Square Diamond Ring Microstrip Filter for WiMAX and WLAN Applications with Negative Group Delay

Bhupendra Dhubkarya[1], Dr. Ratnesh Kumar Jain[2]

[1]*M.Tech. Research Scholar, Department of Electronics & Communication, RKDF University, Bhopal (M.P)*
[2]*Research Guide, Department of Electronics & Communication, RKDF University, Bhopal (M.P)*

ABSTRACT

Because of the rapid increase of wireless and mobile communication in recent decades, the electromagnetic spectrum has become more congested. Compact passband filters with excellent performance are in high demand because of their tiny size in the communications sector. Microstrip filters are now the subject of intense study and development to reduce their size and increase their efficiency. A bandpass filter with closed loop square diamond ring was presented for WLAN and WiMAX applications in this research work. The filter's physical profile is 36mm×24mm in terms of physical dimensions. The filter's substrate is built of FR4 material with a 4.3 dialectic constant and a thickness of 1.6 mm, and it has a complete ground structure. Using a closed-loop square diamond ring, the filter has been constructed. The filter geometry is symmetrical around the x and y-axis. The negative group delay of the proposed tri band bandpass filter makes it more suitable for usage in microwave systems, both in theory and in practice. The filter exhibits insertion loss of 1.1dB, 2.5dB, and 4.8dB and a return loss of 28.7dB, 17.5dB, and 10.53dB in the 2.39GHz, 5.08GHz, and 7.43GHz passbands, respectively. Fractional bandwidths of 13.58%, 6.74%, and 2.3%have been found in this filter. Filter design has a three-transmission zero. The close agreement between the measured and simulated values for the return loss and insertion loss design parameters may be seen in the near similarity of their values.

KEYWORDS

Tri-band, Bandpass filer, microstrip filter, NGD, closed loop, square diamond ring, WLAN, WiMAX.

1. INTRODUCTION

As more and more technologies, such as GSM, WLAN, GPS, RFID, 3G/ 4G/ Bluetooth, and vehicle radar systems, are integrated into a single system, the need for a tiny wireless transceiver for commercial items becomes even more critical [1, 2]. High data rates and a significant quantity of radio frequency spectrum capacity are required for the wireless technologies outlined in [3] as well as other requirements.

Besides being necessary for mobile phones, radio frequency systems are also required for scientific instrumentation, navigation, and even therapeutic applications. It is being attempted to build a compact, low-power component for wireless standards to prevent interfering with the operation of other radio frequency bands. Compact, high-selectivity bandpass filters are a key component of this system since the performance of these filters has an impact on the entire performance of the microwave communication system. In order to achieve this aim, circuit designers must develop multiband BPFs with tiny footprints and little insertion loss, which is a challenging task for them. Microstrip lines with notch bands may be used to enhance upper stopband performance while also providing an amazing pass band feature in the ultra-wideband (UWB) region [4]. A resonator is often employed in filter designs in order to get the required operating band while keeping the filter size as small as possible [5] [6]. For boosting the sharpness of the scattering characteristics, a poor ground structure such as that described in [6] may be a better alternative than a good ground structure. As shown by [7], metamaterial has a considerable impact on the physical characteristics of the filter. Because of their size and excellent loss qualities, hybrid shapes such as circular rings and rectangular stubs are an excellent option for a variety of applications.

Design and construction of a BPF with an acceptable fundamental topology to accomplish this purpose, while operating within the FCC-recommended frequency range in [1]. While rejecting undesirable signals outside of the given range Thick rectangular stubs [8-10] are used in the construction of GSM 1900, WLAN, and WiMAX C-band and X-band BPFs, which improve the edge steepness and

overall performance of the passband while simultaneously shrinking its size. [8-10] Used in WiMAX and WLAN, C-band and X-band satellite applications [11-15], it is coupled to thin I-shaped rectangular stubs with centrally loaded twin tiny inverted-Y stubs to produce quad band responses at 1.918 MHz, 2.411 MHz, and 4.06 GHz, among other frequencies [11-15]. The design concept is tested on an FR4 substrate material to check that the samples that have been suggested are feasible. The relative permittivity of the filter substrate is 4.3, and the dissipation factor of the filter substrate is 0.002. When using the filters, it is possible to adjust their configuration and center frequency by opening and closing various shaped stubs on the filters [17]. Regarding microwave applications, a negative group delay filter is very adaptable and commonly used [18]. Several advantages of multiband bandpass filters have been shown as compared to single-band or quad-band filters [19–21]. To enable tri-band band-pass operation, closed-loop square diamond rings in the symmetrical configuration are employed in the proposed filter design.

2. EVOLUTION OF TRI-BAND FILTER DESIGN

The fundamental tri-band filter configuration with ports and closed loop square diamond is depicted in Figure 1(a). The scattering parameters of the first stage design has been discussed in this section with its corresponding S-parameter vs frequency plot shown in Figure 1(b). The overall volume of the proposed filter is 36×24×1.6 $mm^3$where left edge of the filter has port P_1 (input) and right edge has portP_2(output).

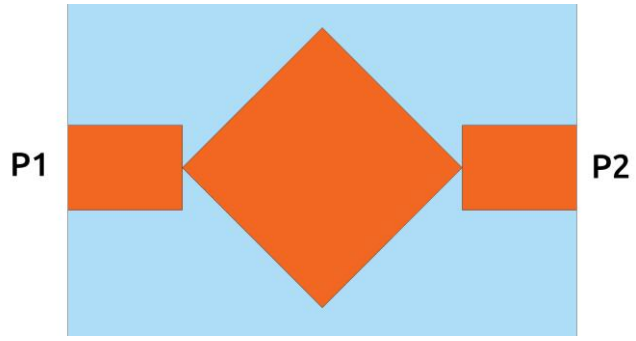

(a)

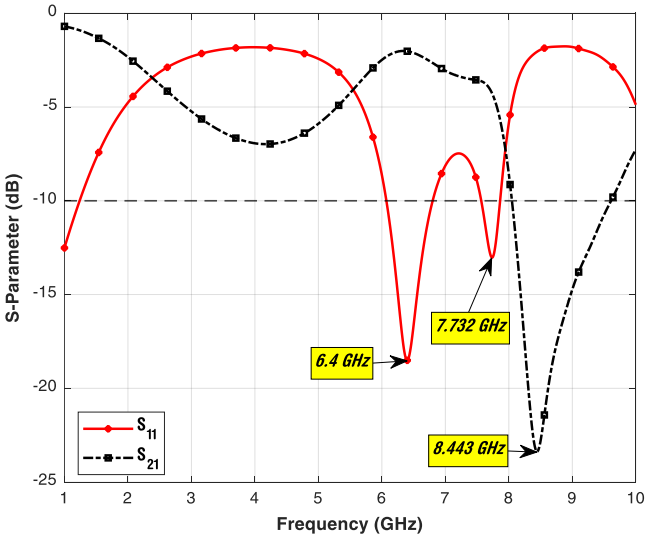

(b)

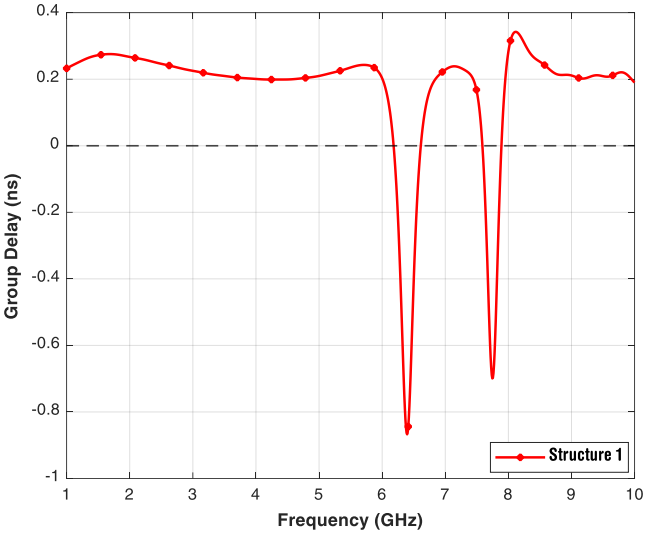

(c)

Figure 1. (a) Layout of the Filter Structure 1, (b) S-parameter curves of Structure 1 and (c) Group Delay of Structure 1

2.1 Filter Evolution Stage 1

In the first design structure, the filter has a rectangular port along with solid square diamond to connect port 1 to port 2 as shown in Figure 1(a). The port is kept higher ratio of width than height. The return loss and insertion loss characteristics of the filter are shown in Figure 1(b) after the excitation. There are two stop bands exhibited by this given structure and resonates on 4.16GHz, and 8.44GHz.The solid square diamond stub creates a mutual field to resonate on passband frequencies of 6.4GHz, and 7.732GHz.This design has only two Transmission Zeros (TZs). The group delay of Structure1 is shown in Figure 1(c) and has negative delay on 6.4GHz and 7.732GHz.

2.2 Filter Evolution Stage 2

The first structure needs some optimization to get near our goal for wireless applications. Therefore, some changes in the design have been incorporated to find Structure2 of the filter. In this design height of the ports, 1 and 2 of the filter is increased keeping the rest of the elements like solid square diamond stub. The geometry has been depicted in Figure 2(a) of filter stage 2. The return loss and insertion loss characteristics of the filter are shown in Figure 2(b) after the excitation.

There are two stop bands exhibited by this Structure2 between 1 to 10GHz and it resonates on 4.429GHz, and 8.551GHz.

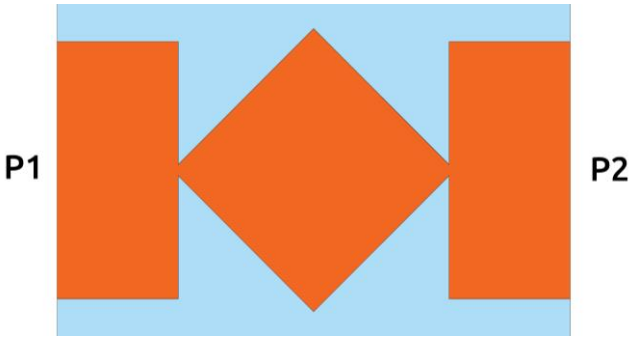

(a)

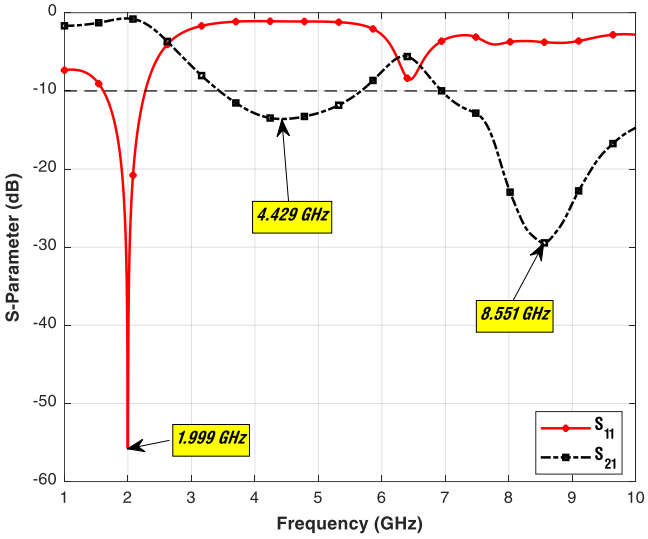

(b)

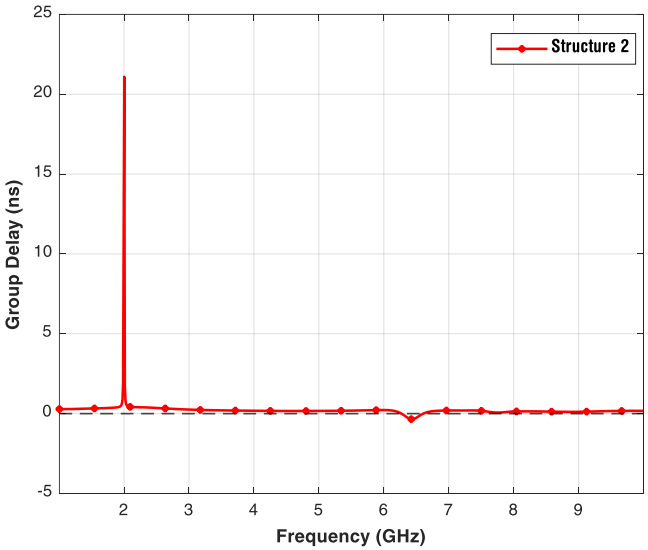

(c)

Figure 2. (a) Layout of the Filter Structure2, (b) S-parameter curves of Structure2 and (c) Group Delay of Structure2

After modification in the port's height symmetrically along y axis, the filter starts resonating on one frequency only 1.999GHz in passband 1 alone. In comparison with the previous structure, the passband $|S_{11}|$ characteristics shifted toward the lower frequency band. This structure also has two TZs. The group delay of Structure2 is shown in Figure 2(c) and has a positive delay throughout the simulated range from 1-10GHz.

2.3 Filter Evolution Stage 3

For the sake of results that are more precise second structure needs to have performed some optimizations. These changes have been incorporated to find Structure3 of the filter. In this design height of the ports 1 and 2 of the filter is kept as Sturcture2 and the inner end of the port is like a square diamond shape. The geometry has been depicted in Figure 3(a). The return loss and insertion loss characteristics of the filter are shown in Figure 3(b) after the excitation.

There are two stop bands exhibited by this Structure3 between 1 to 10GHz and it resonates on 3.943GHz, and 8.434GHz. By making arrow-like shape to the inner side of the ports filter starts resonating on 1.747GHz, and 6.04GHz in the passband. Number of TZs are two in this structure on 3.943GHz and 8.434GHz. The group delay of Structure3 is shown in Figure 3(c) and has negative delay on passband resonating frequencies in the simulated range from 1-10GHz.

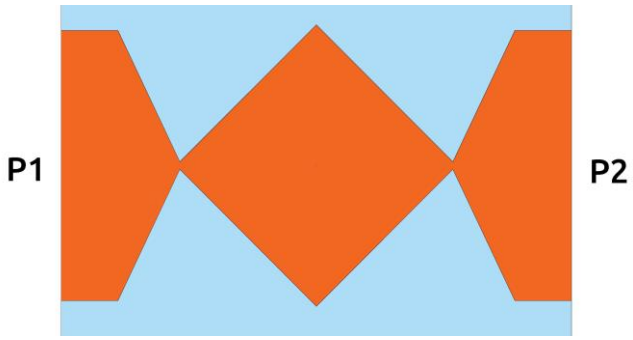

(a)

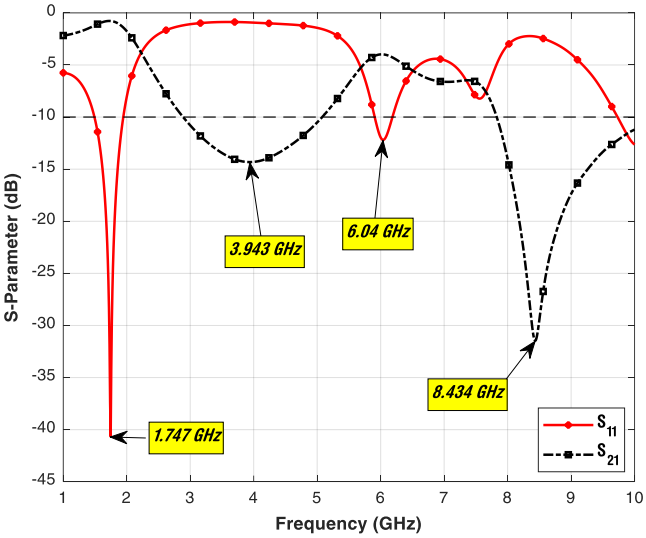

(b)

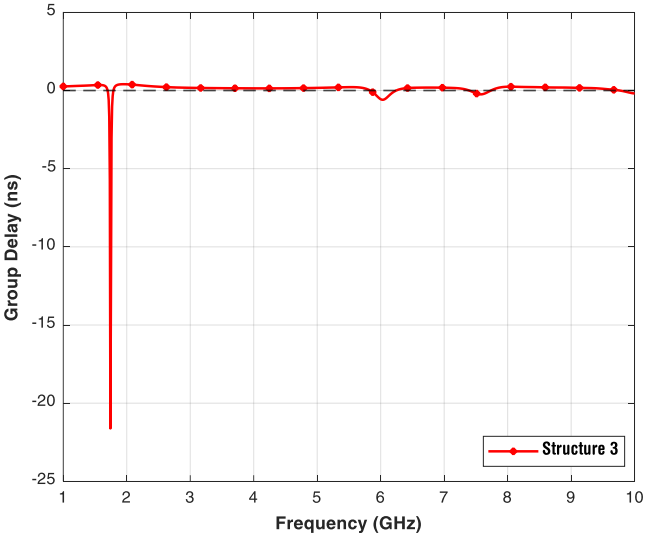

(c)

Figure 3. (a) Layout of the Filter Structure3, (b) S-parameter curves of Structure3 and (c) Group Delay of Structure3

2.4 Filter Evolution Stage 4(Final Filter Geometry)

The final geometry of the filter is achieved as Structure4 after tuning the passband resonance frequencies for consumer wireless applications like WiMAX and WLAN. The tuning in Structure3 has been achieved by making a solid square diamond shape into a ring after introducing a slot into the stub. The dimensions of the diamond-shaped stub are of *So* × *So* width and height at the outer and *Si* × *Si* sized slot inside the diamond stub. The geometry of the final filter design geometry with detailed dimensions is shown in Figure 4(a). The return loss and insertion loss characteristics of the Sturcture4 are shown in Figure 4(b) after the excitation.

This Structure4 between 1 to 10GHz has seen the final pass bands and it resonates on 1.747GHz and 6.04GHz. By making a diamond ring, the pass band frequencies of $|S_{11}|$ parameter are shifted to 2.386GHz, 5.077GHz, and 7.35GHz. The number of TZs is four in this structure. The group delay of Structure4 is shown in Figure 4(c) and has a negative delay on passband resonating frequencies in the simulated range from 1-10GHz. The comparison of return loss and insertion loss characteristics of the filter structure evolution have been compared and shown in Figure 5.

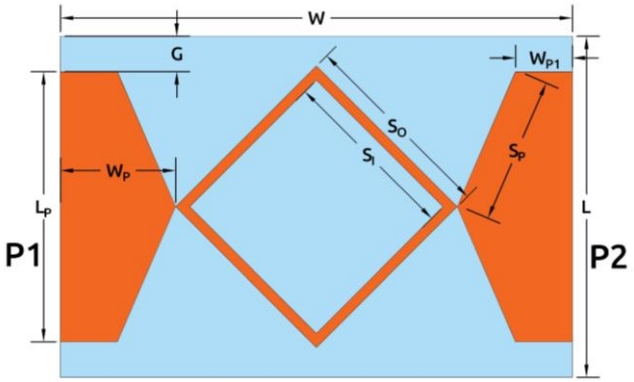

(a)

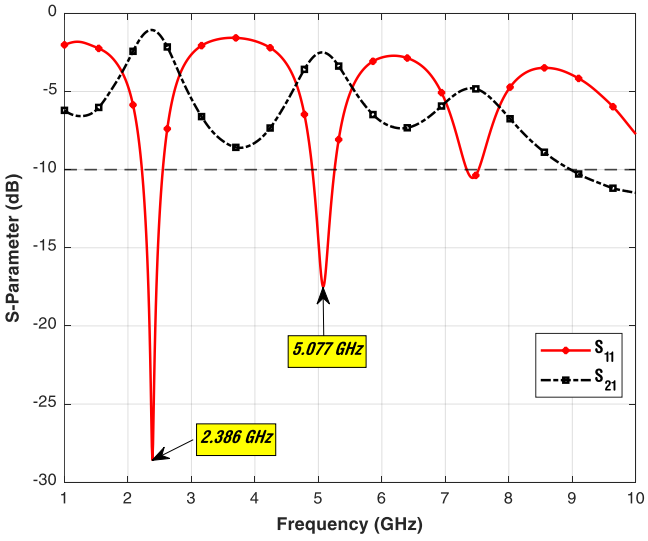

(b)

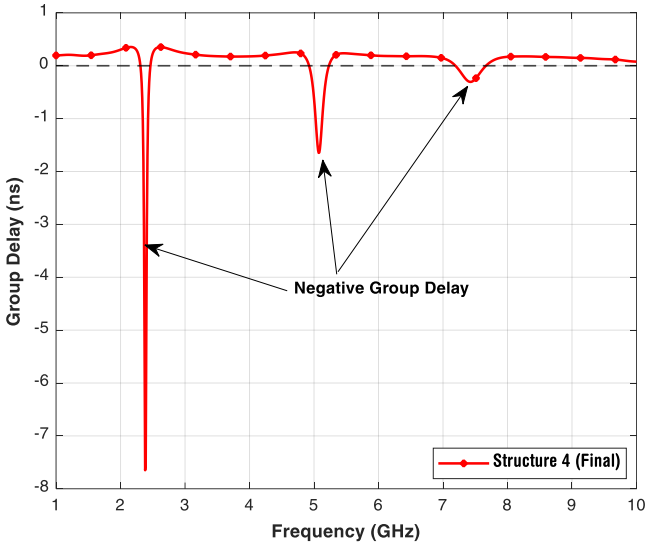

(c)

Figure 4. (a) Optimized Geometry of the Presented Filter Structure4, (b) S-parameter curves of Structure4 and (c) Group Delay of Structure4

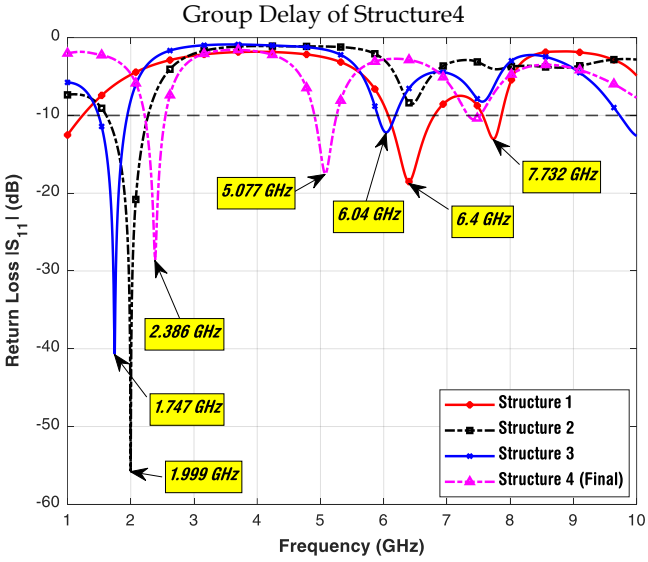

(a)

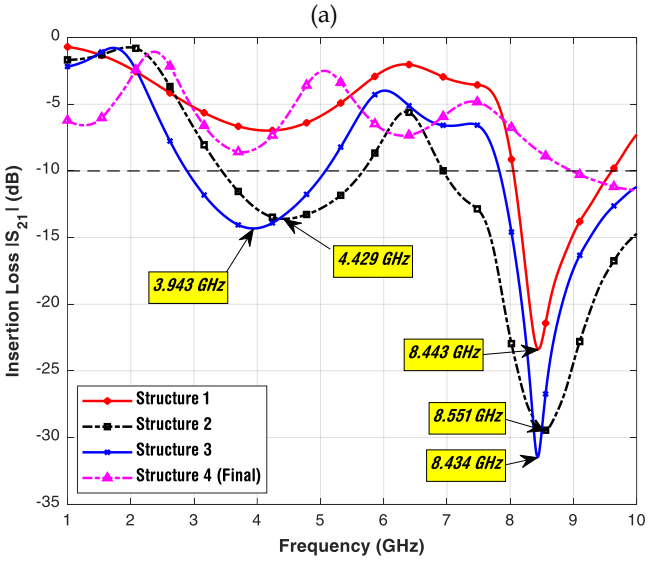

(b)

Figure 5. S-Parameter comparison of Structure1 to 4(a) Return Loss (b) Insertion Loss

Finally, the overall structure of the proposed filter along with square diamond stubs is shown in Figure 6(a). The detailed designed dimension has been given in Table 1.

Table 1. Dimension of Filter

Dimension	Value (mm)	Dimension	Value (mm)
W	36	L	24
W_P	8.1	L_P	19
W_{P1}	4	S_O	14
S_I	12.6	G	2.5

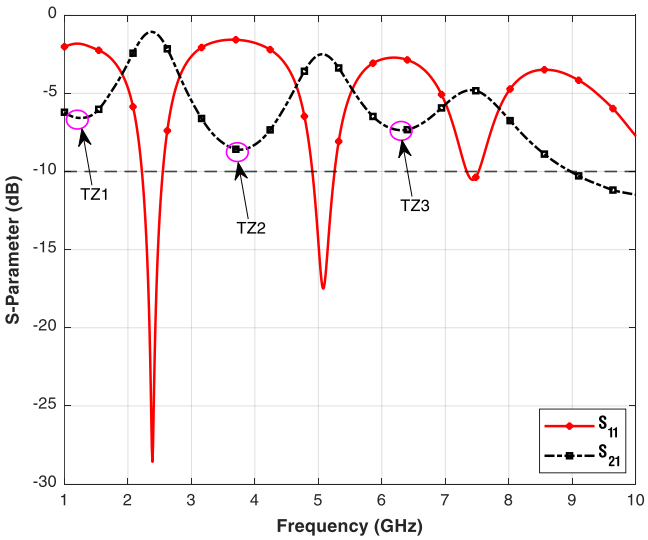

Figure6. All TZs of the proposed filter

3. EXPERIMENTAL RESULT ANALYSIS

Figure 7 depicts the picture of a realized tri-band filter prototype based squared diamond-shaped closed loop placed in symmetry with ports in the xy-axis. The physical size of this bandpass filter is just (36×24) mm², making it more compact than prior designs [15-16],[18],[20], and [23-24]. The suggested filter's reflection coefficient ($|S_{11}|$) and insertion loss ($|S_{21}|$) were tested using an Anritsu vector network analyser.

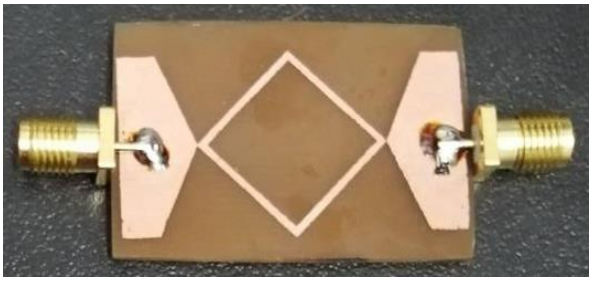

Figure 7. Picture of Realized Triband Square Diamond Ring Fabricated Filter

Figure 8 shows a comparison of the proposed filter's measured and simulated return loss characteristics. It is a graph that compares the experimented and simulated return loss scattering parameters for the proposed tri-band filter with a diamond ring closed loop stub. As shown in Figure 8, the experimental performance has a maximum return loss of -19dB in the pass-band and the simulated response has a reflection coefficient of -28dB in the pass-band. For the target frequency band, both simulated and measured results are in good agreement.

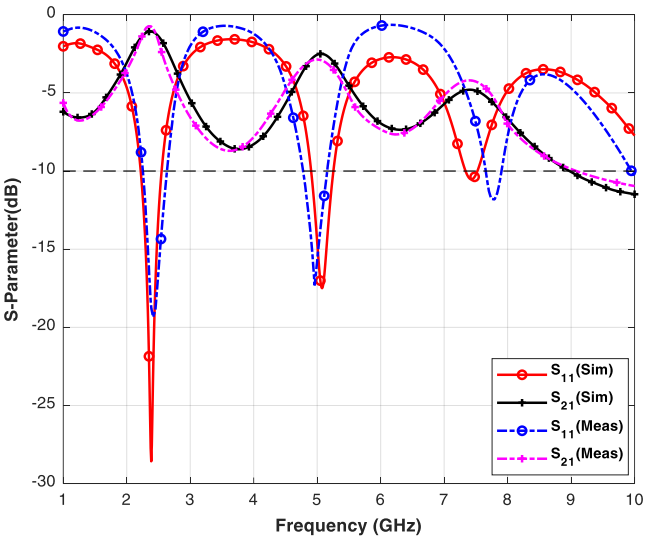

Figure 8. Scattering parameter of the tri-band filter simulation and measured

Figure 8 also shows a comparison between measured and simulated $|S_{21}|$ characteristics. It is a graph comparing the observed and calculated insertion loss for the proposed triband filter with a closed diamond ring closed loop stub. The calculated performance corresponds to a maximum attenuation of -11.15dB in the stop band, while the measured response corresponds to an enhanced maximum attenuation of -10.95dB in the stop band. Figure 6 shows the group delay of the proposed filter, which is in negative. Due to NGD the proposed bandpass filter can be implemented in the feed-forward amplifier circuits and feedback amplifiers which enhances the performance [18] and reduces the physical profile of the circuit.

Table 2 gives the detailed findings of scattering parameters ($|S_{11}|$; $|S_{21}|$) among simulated and measured outcomes e.g., passband, insertion loss, return loss, fractional bandwidth, and transmission zeros of the proposed tri-band filter using two identical line resonators and open-end line stubs.

Table 2. Characteristics comparison of simulation vs measured outcomes of tri band filter

	Passband (GHz)	Insertion Loss (dB)	Return Loss (dB)	FBW (%)	TZ
Simulation	2.39/8.08/7.43	1.06/2.49/4.7	28.57/17.5/10.5	13.58/6.74/2.3	3
Measured	2.44/4.97/7.78	0.7/2.86/4.19	19.34/17.3/11.82	15.07/7.42/3.05	3

Table3. Performance comparison of the filter with previous works

Ref.	Passband (GHz)	Insertion Loss (dB)	Return Loss (dB)	FBW (%)	Size (mm^2)/($\lambda_g \times \lambda_g$)
[15]	2.5/3.4/4.12–5.32	0.37/0.09/0.05	11/19/23	12/21/25	40mm×30.44mm
[18]	1.995	7.5	> 20	-	60mm × 36mm 0.58×0.35
[20]	1.575/2.4/3.45	0.7/1.14/0.3	18/22.3/17	15.8/7.5/5.6	38mm×31mm
[23]	1.51/2.13/2.8	0.74/1.29/1.41	50/25/27	12/7.3/7	108mm × 65mm
Proposed	2.39/8.08/7.43	1.06/2.49/4.7	28.57/17.5/10.5	13.58/6.74/2.3	36mm ×24mm

The proposed tri-band filter has a comparison of performance metrics with previous filter realizations given in Table 3. The proposed filter design has tri bands of operation while maintaining the lower physical profile of 25×16 mm^2. The fractional bandwidth is better than [15],[18], [20] and [23].

4. CONCLUSION AND FUTURE SCOPE

Great-performance passband filters are in high demand in communications because they are small and work well. Researchers are looking at new ways to construct compact microstrip filters to boost their performance and shrink their overall filter size. We were able to create and test a small filter design in this piece of work. It may be inferred that the suggested filter design can function for four bands based on the results of the experiment. According to Table 3, it is also smaller than its rivals in terms of physical dimensions. This work provided a closed-loop diamond ring-shaped tri-band bandpass filter for WLAN and WiMAX applications. The filter's dimensions are 36mm×24mm. The substrate is made of FR4 and has a dialectic constant of 4.3 and a thickness of 1.6 millimeters. Asymmetry is avoided by aligning the closed-loop diamond ring stub. The negative group delay of the tri-band bandpass filter under consideration makes it more suitable for use in microwave systems. On 2.39GHz, 8.08GHz, and 7.43GHz, insertion loss is 1.06dB, 2.49dB, and 4.7dB, while return loss is 28.57dB, 17.5dB, and 10.5dB. Fractional bandwidths of 13.58%, 6.74%, and 2.3% are all good for the filter. Three TZs are found for use in the filter. An excellent agreement in the design parameters may be shown by comparing the measured and predicted return and insertion loss values. The DGS technique may be used to further improve this design by adjusting the frequency of desired processes. Pass and stop bands may be added by integrating resonators. Furthermore, the device's size may be further reduced by the use of a different substrate material. It is possible to use the suggested bandpass filter in the feed-forward amplifier and feedback amplifier circuits, which improves performance and reduces the circuit's physical profile.

REFERENCES

[1] FCC, 'Revision of part 15 of the commission's rules regarding ultra-wideband transmission systems'. Tech. Rep. ETDocket 98–153, FCC02-48, Federal Communications Commission, 2002.

[2] T. George and B. Lethakumary, 'High frequency rejection using L shaped defected microstrip structure in ultra wideband bandpass filter', *Materials Today: Proceedings*, vol. 25, pp. 265–268, 2020, doi: 10.1016/j.matpr.2020.01.363.

[3] C.-Y. Hung, M.-H. Weng, Y.-K. Su, R.-Y. Yang, and H.-W. Wu, 'Design of Compact and Sharp-Rejection Ultra Wideband Bandpass Filters Using Interdigital Stepped-Impedance Resonators', *IEICE Transactions on Electronics*, vol. E90-C, no. 8, pp. 1652–1654, Aug. 2007, doi: 10.1093/ietele/e90-c.8.1652.

[4] S. W. Wong and L. Zhu, 'Implementation of Compact UWB Bandpass Filter With a Notch-Band', *IEEE Microw. Wireless Compon. Lett.*, vol. 18, no. 1, pp. 10–12, Jan. 2008, doi: 10.1109/LMWC.2007.911972.

[5] A. Belmajdoub, A. E. Alami, S. Das, B. T. P. Madhav, S. D. Bennani, and M. Jorio, 'Design, optimization and realization of compact bandpass filter using two identical square open-loop resonators for wireless communications systems', *J. Inst.*, vol. 14, no. 09, pp. P09012–P09012, Sep. 2019, doi: 10.1088/1748-0221/14/09/P09012.

[6] J. Liu, W. Ding, J. Chen, and A. Zhang, 'New Ultra-Wideband Filter with Sharp Notched Band Using Defected Ground Structure', *PIER Letters*, vol. 83, pp. 99–105, 2019, doi: 10.2528/PIERL18111302.

[7] D. K. Choudhary and R. K. Chaudhary, 'A Compact via-Less Metamaterial Wideband Bandpass Filter Using Split Circular Rings and Rectangular Stub', *PIER Letters*, vol. 72, pp. 99–106, 2018, doi: 10.2528/PIERL17092503.

[8] A. Basit, M. I. Khattak, and M. Alhassan, 'Design and Analysis of a Microstrip Planar UWB Bandpass Filter with Triple Notch Bands for WiMAX , WLAN, and X-Band Satellite Communication Systems', *PIER M*, vol. 93, pp. 155–164, 2020, doi: 10.2528/PIERM20042602.

[9] C. Karpuz, A. K. Gorur, and E. Sahin, 'Dual-mode dual-band microstrip bandpass filter with controllable center frequency', *Microw. Opt. Technol. Lett.*, vol. 57, no. 3, pp. 639–642, Mar. 2015, doi: 10.1002/mop.28914.

[10] R. Gomez-Garcia, J.-M. Munoz-Ferreras, W. Feng, and D. Psychogiou, 'Balanced Symmetrical Quasi-Reflectionless Single-and Dual-Band Bandpass Planar Filters', *IEEE Microw. Wireless Compon. Lett.*, vol. 28, no. 9, pp. 798–800, Sep. 2018, doi: 10.1109/LMWC.2018.2856400.

[11] L.-T. Wang, Y. Xiong, L. Gong, M. Zhang, H. Li, and X.-J. Zhao, 'Design of Dual-Band Bandpass Filter With Multiple Transmission Zeros Using Transversal Signal Interaction Concepts', *IEEE Microw. Wireless Compon. Lett.*, vol. 29, no. 1, pp. 32–34, Jan. 2019, doi: 10.1109/LMWC.2018.2884147.

[12] R. Gomez-Garcia, L. Yang, J.-M. Munoz-Ferreras, and D. Psychogiou, 'Selectivity-Enhancement Technique for Stepped-Impedance-Resonator Dual-Passband Filters', *IEEE Microw. Wireless Compon. Lett.*, vol. 29, no. 7, pp. 453–455, Jul. 2019, doi: 10.1109/LMWC.2019.2916458.

[13] B. Ren *et al.*, 'Compact Dual-Band Differential Bandpass Filter Using Quadruple-Mode Stepped-Impedance Square Ring Loaded Resonators', *IEEE Access*, vol. 6, pp. 21850–21858, 2018, doi: 10.1109/ACCESS.2018.2829025.

[14] M.-H. Weng, S.-W. Lan, S.-J. Chang, and R.-Y. Yang, 'Design of Dual-Band Bandpass Filter With Simultaneous Narrow- and Wide-Bandwidth and a Wide Stopband', *IEEE Access*, vol. 7, pp. 147694–147703, 2019, doi: 10.1109/ACCESS.2019.2946302.

[15] T. A. Sheikh, J. Borah, and S. Roy, 'Design of compact bandpass filter for WiMAX and UWB application using asymmetric SIRs and DGS', *Radioelectron.Commun.Syst.*, vol. 59, no. 6, pp. 269–273, Jun. 2016, doi: 10.3103/S0735272716060066.

[16] M. Mabrok, Z. Zakaria, Y. E. Masrukin, T. Sutikno, and H. Alsariera, 'Effect of the defected microstrip structure shapes on the performance of dual-band bandpass filter for wireless communications', *Bulletin EEI*, vol. 10, no. 1, pp. 232–240, Feb. 2021, doi: 10.11591/eei.v10i1.2662.

[17] G.-Z. Liang and F.-C. Chen, 'A Compact Dual-Wideband Bandpass Filter Based on Open-/Short-Circuited Stubs', *IEEE Access*, vol. 8, pp. 20488–20492, 2020, doi: 10.1109/ACCESS.2020.2968518.

[18] Z. Wang, Z. Fu, C. Li, S.-J. Fang, and H. Liu, 'A Compact Negative-Group-Delay Microstrip Bandpass Filter', *PIER Letters*, vol. 90, pp. 45–51, 2020, doi: 10.2528/PIERL19122701.

[19] Z. Gao, P. Wu, and Y. Zhang, 'A New Compact Microstrip Ultra-Wideband (UWB) Bandstop Filter with Good Performance', *PIER Letters*, vol. 93, pp. 9–12, 2020, doi: 10.2528/PIERL20052304.

[20] M. Rahman and J.-D. Park, 'A Compact Tri-Band Bandpass Filter Using Two Stub-Loaded Dual Mode Resonators', *PIER M*, vol. 64, pp. 201–209, 2018, doi: 10.2528/PIERM17120404.

[21] K. G. Avinash and I. Srinivasa Rao, 'Compact dual-band bandpass filter based on dual-mode modified star shaped resonator', *Microw. Opt. Technol. Lett.*, vol. 59, no. 3, pp. 505–511, Mar. 2017, doi: 10.1002/mop.30333.

[22] C. Kim, T. Hyeon Lee, B. Shrestha, and K. Chul Son, 'Miniaturized dual-band bandpass filter based on stepped impedance resonators', *Microw. Opt. Technol. Lett.*, vol. 59, no. 5, pp. 1116–1119, May 2017, doi: 10.1002/mop.30481.

[23] R. Gomez-Garcia, R. Loeches-Sanchez, D. Psychogiou, and D. Peroulis, 'Multi-Stub-Loaded Differential-Mode Planar Multiband Bandpass Filters', *IEEE Trans. Circuits Syst. II*, vol. 65, no. 3, pp. 271–275, Mar. 2018, doi: 10.1109/TCSII.2017.2688336.

[24] Z. Yang, B. You, and G. Luo, 'Dual−/tri-band bandpass filter using multimode rectangular SIW cavity', *MicrowOpt Technol Lett*, vol. 62, no. 3, pp. 1098–1102, Mar. 2020, doi: 10.1002/mop.32145.

[25] F. Zhao, M. Weng, C. Tsai, R. Yang, H. Lai, and S. Liu, 'A miniaturized high selectivity band-pass filter using a dual-mode patch resonator with two pairs of slots', *MicrowOpt Technol Lett*, vol. 62, no. 3, pp. 1145–1151, Mar. 2020, doi: 10.1002/mop.32165.